Phase correlation based image alignment with subpixel accuracy

Alfonso Alba, Ruth M. Aguilar-Ponce, J. Flavio Vigueras-Gómez, and Edgar Arce-Santana

Facultad de Ciencias, Universidad Autónoma de San Luis Potosí,
Av. Salvador Nava Mtz. S/N, Zona Universitaria, 78290, San Luis Potosí, SLP,
México.
E-mail: fac@fc.uaslp.mx (A. Alba), rmariela@fciencias.uaslp.mx (R.M.
Aguilar-Ponce), flavio@fc.uaslp.mx (J.F. Vigueras-Gómez),
arce@fciencias.uaslp.mx (E. Arce-Santana)

Abstract. The phase correlation method is a well-known image alignment technique with broad applications in medical image processing, image stitching, and computer vision. This method relies on estimating the maximum of the phase-only correlation (POC) function, which is defined as the inverse Fourier transform of the normalized cross-spectrum between two images. The coordinates of the maximum correspond to the translation between the two images. One of the main drawbacks of this method, in its basic form, is that the location of the maximum can only be obtained with integer accuracy. In this paper, we propose a new technique to estimate the location with subpixel accuracy, by minimizing the magnitude of gradient of the POC function around a point near the maximum. We also present some experimental results where the proposed method shows an increased accuracy of at least one order of magnitude with respect to the base method. Finally, we illustrate the application of the proposed algorithm to the rigid registration of digital images.

1 Introduction

The phase correlation method [1] is a frequency domain technique used to estimate the delay or shift between two copies of the same signal. This technique is based on the shift properties of the Fourier transform. Specifically, consider two discrete periodic signals $f(x)$ and $g(x)$, and let $F(\omega)$ and $G(\omega)$ be their respective Fourier transforms. The normalized cross-spectrum $R(\omega)$ of f and g is given by

$$R(\omega) = \frac{F(\omega)G^*(\omega)}{|F(\omega)G^*(\omega)|}, \tag{1}$$

where G^* is the complex conjugate of G. Note that $|R(\omega)| = 1$ for all ω. Also, the phase-only correlation (POC) function $r(x)$ is defined as the inverse Fourier transform of $R(\omega)$.

Now suppose g is simply a delayed copy of f; that is, $g(x) = f(x + d)$, where d is an unknown integer. The shift property of the Fourier transform states

that $G(\omega) = F(\omega) \exp\{j\omega d\}$, where $j = \sqrt{-1}$. In this case, it is easy to see that $R(\omega) = \exp\{-j\omega d\}$ and $r(x) = \delta(x-d)$, where δ is the discrete impulse function (i.e., $\delta(0) = 1$ and $\delta(x) = 0$ for $x \neq 0$). Therefore, one can recover d by simply locating the maximum of $r(x)$.

This method can be easily extended to 2D and 3D images, and has been successfully applied in several image processing and computer vision problems, such as image registration [2], [3], [4], [5], biometrics [6], [7], [8], stereo disparity estimation [9] [10], motion and optical flow estimation [11], [10], and video encoding [12], [10].

One of the most important drawbacks of the phase correlation method, at least in its basic form, is that the recovered displacements have integer accuracy; i.e., the coordinates of the maximum of the discrete POC function will be a rounded version of the components of the true displacement vector. Various alternatives have been devised to estimate the displacements with non-integer (subpixel) accuracy. Among the most popular are those which rely on local function fitting: one can first obtain the displacement d_0 with integer accuracy using the basic phase correlation method and fit a simple analytical function $f(d)$ (e.g., a polynomial) to the POC values in a neighborhood of d_0; then one maximizes $f(d)$ to estimate the true maximum. The most common fitting functions are quadratic polynomials and Gaussian functions [13], cubic splines [6], and Dirichlet or sinc functions [14], [15], [11]. Most of these methods perform reasonably well under controlled conditions but their performance is seriously degraded by noise, border effects, and the presence of multiple motions. This limits the application of these methods to many computer vision problems, such as stereo depth or optical flow estimation.

In this paper, we introduce a new method for the estimation of POC maxima with subpixel accuracy, which is based on finding approximate zeros of the gradient of the POC function. The proposed method, which is presented in Section 2, is capable of high-accuracy estimations while maintaining adequate robustness to noise and multiple motions. In Section 3, we use synthetic data to demonstrate the advantages of our method for the estimation of rigid image transformations. Finally, our conclusions are presented in Section 4.

2   Methodology

Instead of relying on local function fitting, the proposed method attempts to estimate the POC maxima by finding approximate zeros of the POC gradient near the integer-valued displacements. Throughout rest of the article, we will use square brackets to denote N-periodic discrete-time signals (e.g., $f[x]$, where $x = 0, \ldots, N_x - 1$), and parentheses for continuous-time signals (e.g., $f(x)$ with $x \in \mathbb{R}$). Also note that in most cases we will be dealing with periodic signals and will obviate the need of mod-N indexing (e.g., $f[x + N] = f[x]$).

2.1   Gradient estimation of the POC function

Consider again the 1D case of the POC function $r[x]$, which is defined as the inverse discrete Fourier transform of the normalized cross-correlation $R[k]$; in other words,

$$r[x] = \sum_{k=0}^{N-1} R[k] \exp \{2\pi jkx/N\}, \tag{2}$$

where N is the period of the signals.

The right-hand side of the above equation provides, in fact, a band-limited, continuous representation of the phase correlation function. By differentiating this expression with respect to x, one can obtain an analytical, continuous expression of the derivative of the POC function $r'(x)$, which is given by

$$r'(x) = j\frac{2\pi}{N} \sum_{k=0}^{N-1} kR[k] \exp \{2\pi jkx/N\}. \tag{3}$$

Note that, for real-valued input signals $f(x)$ and $g(x)$, the POC function is also real, so its derivatives must be real as well. This means one can also compute $r'(x)$ as

$$r'(x) = -\frac{2\pi}{N} \sum_{k=0}^{N-1} k \ \Im \{R[k] \exp \{2\pi jkx/N\}\}, \tag{4}$$

which in some cases may be computationally more efficient.

The problem of finding the extrema of the POC function with sub-pixel accuracy is equivalent to finding the zeros of $r'(x)$. In 1D, the approach is straightforward: use the integer-valued displacement obtained from the discrete POC function as a starting point for a root-finding algorithm such as bisection or Newton-Raphson (the second derivative of the POC, required for Newton-Raphson, is also easy to obtain, although somewhat unstable). However, generalizing this idea to 2D (or higher dimensions) carries some difficulties. Since the POC function is now bivariate (e.g., $r(x,y)$), its derivative takes the form of a vector-valued bivariate gradient function, given by

$$\nabla r(x,y) = \left[\frac{\partial r}{\partial x}(x,y), \ \frac{\partial r}{\partial y}(x,y) \right], \tag{5}$$

with

$$\frac{\partial r}{\partial x}(x,y) = -\frac{2\pi}{N_x} \sum_{l=0}^{N_y-1} \sum_{k=0}^{N_x-1} k \ \Im \left\{ R[k,l] \exp \left\{ 2\pi j \left(\frac{kx}{N_x} + \frac{ly}{N_y} \right) \right\} \right\}, \tag{6}$$

and

$$\frac{\partial r}{\partial x}(x,y) = -\frac{2\pi}{N_y} \sum_{l=0}^{N_y-1} \sum_{k=0}^{N_x-1} l \ \Im \left\{ R[k,l] \exp \left\{ 2\pi j \left(\frac{kx}{N_x} + \frac{ly}{N_y} \right) \right\} \right\}, \tag{7}$$

where N_x and N_y are, respectively, the width and height of the input images.

Instead of finding the zeros of $\nabla r(x, y)$, one can approximate them by minimizing the real-valued magnitude of the gradient. In other words, the estimated displacement (d_x, d_y) is given by

$$(d_x, d_y) = \arg \min_{(x,y) \in \mathcal{N}(x_0, y_0)} h(x, y), \tag{8}$$

where $h(x, y) = |\nabla r(x, y)|^2$, (x_0, y_0) is a suitable initial solution (e.g., the integer-valued displacement estimation), and $\mathcal{N}(x_0, y_0)$ is a neighborhood centered at this point.

2.2   Minimization of gradient magnitude

Equation 3 shows that the spectrum of the derivative of the POC function is obtained as the normalized cross-spectrum $R[k]$ multiplied by the frequency k. This means that $r'(x)$ will, in general, have an increased high-frequency content with respect to $r(x)$. If one were to compute the second derivative $r''(x)$, it would show even more high-frequency content, making it very sensitive to noise and border effects. For this reason, we have chosen to avoid methods based on the derivatives of $h(x, y)$ (i.e., the second-order derivatives of the POC function) such as gradient or Newton descent methods. Instead, we have chosen two methods which rely only on the evaluation of the function to be optimized.

Grid search.-   The initial solution (x_0, y_0) is refined by evaluating $h(x, y)$ at the nodes of a $(2n+1) \times (2n+1)$ grid centered at (x_0, y_0), with a spacing of w units between adjacent nodes. The node $(\hat{x}, \hat{y})$ with the lowest h is chosen as the best solution. Further refinement is obtained by reducing w and iterating the method with $(\hat{x}, \hat{y})$ as the new center point. We have obtained good results after 2 or 3 iterations with n between 5 and 10. The initial spacing is $w = 1/(2n)$ so that the initial search area covers exactly 1 pixel; after each iteration, w is divided by n, restricting the search to an area equivalent to one cell of the previous grid.

Nelder-Mead optimization.-   The Nelder-Mead method [16] is a well-known minimization heuristic which relies only on the evaluation of the function to be minimized. In order to minimize a function f of n variables, the method requires $n + 1$ points, $x_1, \ldots, x_{n+1} \in \mathbb{R}^n$ forming a simplex (i.e., no two points can be colinear). The method works iteratively by selecting the worst point in the set; that is, a point x_h such that $f(x_i) \leq f(x_h)$ for $i = 1, \ldots, n$, and replacing it by a new, better point x_0, which lies along the line defined by x_h and the centroid of the remaining n points. Depending on how good the new point is with respect to the given points, it can be reflected, expanded, or contracted along the line (see [16]). When applying this method to minimize the POC gradient $h(x, y)$ one requires 3 starting points; the first one is the integer solution (x_0, y_0), and the remaining two were chosen as $(x_0 \pm 0.5, y_0)$ and $(x_0, y_0 \pm 0.5)$ where the sign was selected depending on which neighbor was best. The results were very similar

to the grid search method; however, many less points were evaluated with the Nelder-Mead approach, making it computationally more efficient. The reflection, expansion, and contraction coefficients we used were $\alpha = 1$, $\gamma = 2$, and $\beta = 0.5$, respectively, and the method usually converged in less than 100 iterations.

2.3 Bandlimited phase correlation

Most of the methods which attempt to estimate the maxima of the POC function [14], [17], [15] with subpixel accuracy are seriously affected by noise, aliasing, and border effects, which are mostly present in the higher components of the frequency spectrum of the signals. Therefore, it is strongly suggested to limit the bandwidth of the POC function prior to the estimation of the POC maxima. In many cases, a simple ideal lowpass filter is sufficient and very easy to implement, since it only requires zeroing those coefficients in $R[k]$ corresponding to higher frequencies, before taking its inverse Fourier transform. In the proposed method, we can apply this filter directly in the estimation of the partial derivatives (Eqs. 6 and 7) by summing only those terms with $k < \kappa N_x$ and $l < \kappa N_y$, where κ represents the cutoff frequency of the filter and must be between 0 and 0.5. In our tests, good results were obtained with $\kappa \approx 0.3$.

2.4 Application to rigid image registration

To demonstrate the applicability of the proposed method, we have implemented a rigid image registration algorithm based on the one proposed by Reddy et al. [3], with the exception that the POC maxima are estimated with sub-pixel accuracy. By definition, a rigid transformation is composed only of rotations and translations; however, the proposed algorithm can also deal with isotropic scalings (equal scaling along all axes), and could be easily extended to 3D images (e.g., MRI volumes). This algorithm can be summarized in the following steps (see [3] for details):

1. Let I_1 and I_2 be the input images of equal size, where I_2 is assumed to be a rigidly transformed version of I_1.
2. Compute the discrete Fourier transform $\hat{I}_k$ of each input image I_k.
3. Compute the log-magnitude of the spectra M_k of each image as

$$M_k[k,l] = W[k,l] \log \left| \hat{I}_k[k,l] \right|, \tag{9}$$

   where $W[k,l]$ is the frequency response of a high-pass filter. Here we use the one suggested by Reddy, which is given by $W[k,l] = (1 - X[k,l])(2 - X[k,l])$ with $X[k,l] = \cos(\pi k/N_x) \cos(\pi l/N_y)$ for $-N_x/2 \le k < N_x/2$ and $-N_y/2 \le l < N_y/2$. It can be shown that M_k is invariant to translation.
4. Transform M_k from cartesian coordinates $[x,y]$ to log-polar coordinates $[\rho, \theta]$, where $\rho = K\sqrt{x^2 + y^2}$, $\theta = \text{atan2}(y,x)$, and K is an adequate scaling factor which controls the resolution of the radius (ρ) axis. We have obtained good results with $K = (N_x + N_y)/8$, where $N_x \times N_y$ is the size of the input images.

5. Compute the normalized cross-correlation $R_M[k,l]$ and the POC function $r_M[\rho,\theta]$ between $M_1[\rho,\theta]$ and $M_2[\rho,\theta]$.
6. Estimate the maximum of r_M with subpixel accuracy using the proposed method. The coordinates of this maximum correspond to the scaling and rotation parameters (s and ϕ, respectively) between I_1 and I_2.
7. Let $\tilde{I}_1[x,y] = I_1(T_{s,\phi}\{x,y\})$, where $T_{s,\phi}$ is a transformation defined as

$$T_{s,\phi}\{x,y\} = \begin{bmatrix} s\cos\phi & -s\sin\phi \\ s\sin\phi & s\cos\phi \end{bmatrix} \begin{bmatrix} x \\ y \end{bmatrix}. \qquad (10)$$

In other words, $\tilde{I}_1$ is a rectified version of I_1, rotated and scaled according to the parameters found in the previous step.
8. Compute the normalized cross-correlation $R[k,l]$ and the POC function $r[x,y]$ between $\tilde{I}_1$ and I_2.
9. Estimate the maximum of r with subpixel accuracy. The coordinates of the maximum correspond to the translation between the input images.

3   Results and discussion

In this section we present some results obtained with the application of our approach to different image registration situations. To evaluate the accuracy of the registrations, we take a reference image and perform an artificial transformation with known parameters. The reference and transformed images are then registered, and the estimated parameters are compared against the true ones using the True Mean Relative Error (TRME) [18], defined as

$$\text{TRME} = \frac{1}{4}\left[\frac{s-\hat{s}}{s} + \frac{\phi-\hat{\phi}}{\phi} + \frac{d_x-\hat{d}_x}{d_x} + \frac{d_y-\hat{d}_y}{d_y}\right], \qquad (11)$$

where (s,ϕ,d_x,d_y) are the true parameters and $(\hat{s},\hat{\phi},\hat{d}_x,\hat{d}_y)$ the estimated ones. Note that this error measure is more sensitive to accuracy when the transformation parameters are relatively small.

3.1   Optimization approaches

In the first set of experiments we compared the performance of the original phase correlation approach with integer accuracy, and the subpixel grid search optimization approach and the Nelder-Mead simplex method.

A set composed of 100 affine transformations was generated assigning random values for the scale s, 2D rotation ϕ, and for the translation vector (d_x,d_y). These values were sampled uniformly in the following way: s in the interval $(2^{-0.5},2^{0.5})$, ϕ in the interval $(-30°,30°)$, d_x and d_y both in the interval $(-32,32)$ (pixels). A 260×260 T1 MRI image (Fig. 1(a)) was used for registration. Reference images were created applying the 100 affine transformations described above to the original image and then computing the estimated transformation through
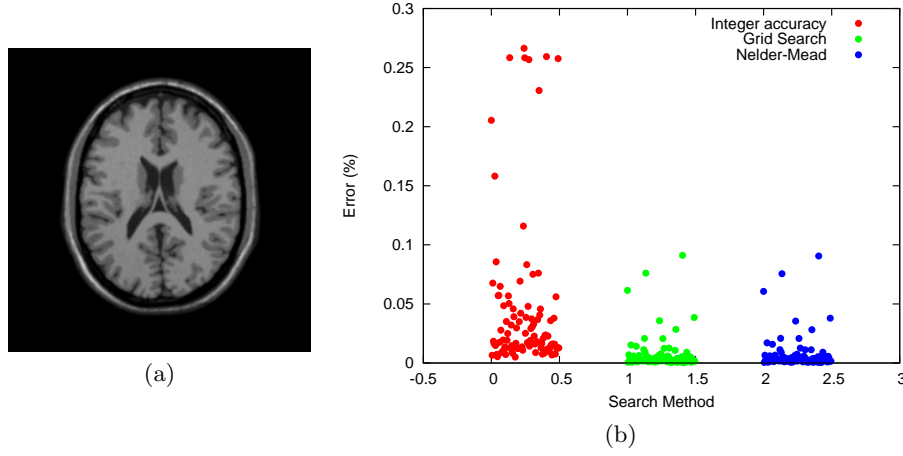
Fig. 1. (a) T1 MRI reference image used for registration tests; a test case is generated by applying a random transformation to this image. (b) TRME error for each test case and each registration method.

the approach presented in this paper. Fig. 1(b) shows the relative errors for all the transformations estimated through the (a) POC with integer accuracy, (b) subpixel grid search, and (c) Nelder-Mead subpixel optimization as they were described in Section 2. Errors between the grid search and the Nelder-Mead optimization are very similar and, both of them are smaller than the original POC approach with integer accuracy.

We consider a *successful estimation* if the corresponding relative error was at most 0.1, and we compute the average and the median of all the successful estimations for the three approaches, and the computation time for each one (see Table 1). Success mean errors and success median errors are almost the same for the grid search and Nelder-Mead approaches and they are much smaller than the corresponding values with integer accuracy. The success rate error was also improved from 90% at the integer accuracy approach to 100% in the other two approaches. Nevertheless, the main difference between the Grid Search and Nelder-Mead is the overhead computation time: Nelder-Mead required in average 10.6ms (in addition to the basic POC search method) to get a solution similar to the one recovered by Grid Search in 184.4ms in this experiment. For this reason, we have conducted the rest of our experiments using only the Nelder-Mead optimization.

3.2   Robustness against transformation complexity

Nine sets composed of 100 affine transformations were generated assigning random values for the transformation parameters. These values were sampled uniformly in the following way: s in the interval $(1 - 0.1a, 1 + 0.1a)$, ϕ in the interval $(-10a, 10a)$ (degrees), d_x and d_y both in the interval $(-10a, 10a)$ (pixels), where

Search method	Success rate	Success mean error	Success median error	Average time (ms)
Integer accuracy	90%	2.74947%	1.93281%	125.5
Grid Search	100%	0.700544%	0.287313%	309.9
Nelder-Mead	100%	0.700457%	0.292196%	136.1

Table 1. Results obtained after 100 synthetic registration cases using the three methods under discussion.

$a = 1, \cdots, 9$ (each value of a corresponds to one of the nine sets). The a-th set is called the tranformation complexity of level a. Transformations with higher complexity are more difficult to be successfully estimated because of possibly small scale factors, or because parts of the transformed image may be cropped when they lie outside of the image frame, producing artificial borders and loss of data.

Fig. 2(a) shows the graph of success rate with respect to the complexity of the affine transformations. It is observed that subpixel approach based on Nelder-Mead optimization always improve the success rate with integer accuracy, and this rate suddenly decreases after level 6. Fig. 2(b) shows that success improvement is better for low complexity transformations. Due to the fact that we use a relative measurement of the error, it seems logical that the relative error seems large for low complexity transformations although the absolute error is still proportional to the transformation parameters.

In Fig. 2(c), the median and average errors are shown for both approaches: integer accuracy and Nelder-Mead. In both approaches, average error is under the threshold of 0.1 relative error and it increases for complexity level 6 and larger, and Nelder-Mead always improve the error with respect to the integer accuracy POC. Moreover, median error remains under the threshold of 0.05 of relative error up to level 7, i.e. more than 50% of the tests are under this threshold although the average error increases significatively (some estimations are very far from the expected values).

Fig. 2(d) shows that the improvement on the True Relative Mean Error (TRME) is better for complexity levels 1 to 3, although the improvement is still noticeable up to level 6. For this experiment, the improvement ratio on the best subpixel TRME is approximately 0.2 times the TRME obtained with integer accuracy, while the improvement ratio on the median of the error is almost constant for levels 1 to 8, being 0.15 times the median obtained with integer accuracy.

3.3   Robustness to noise and missing data

In order to test the robustness of the method against noise, we consider additive noise with Gaussian distribution, which was added to the transformed image. Then, we vary the standard deviation from 0 to 0.3 in a normalized scale (i.e., the gray levels go from 0 to 1). The true transformation was fixed with the
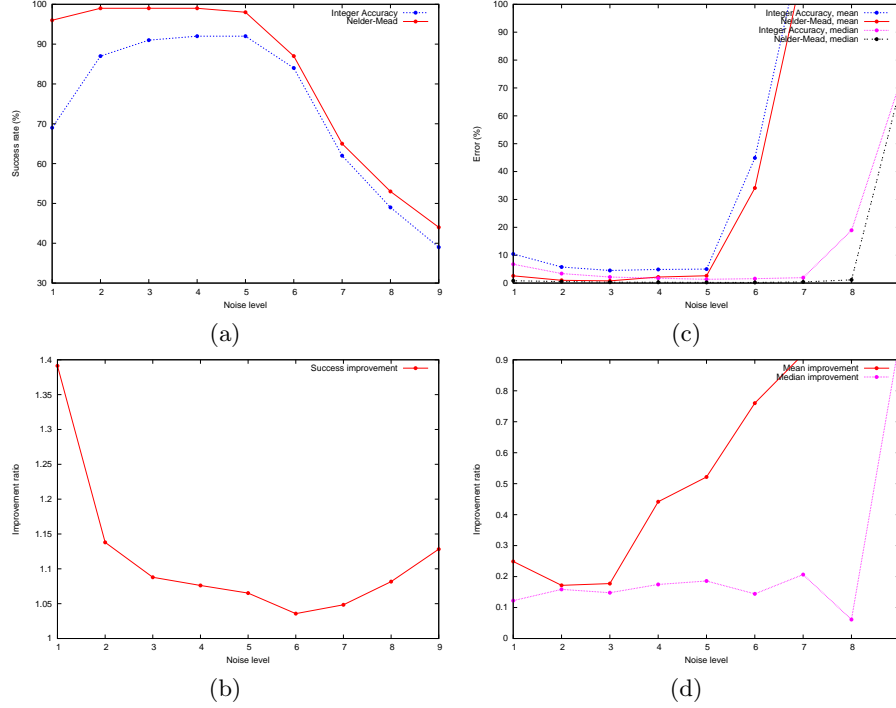
Fig. 2. Results obtained with transformations of varying complexity: (a) success rate, (b) success improvement ratio, (c) mean and median error, (d) mean and median error improvement ratio. See text for details.

following values: horizontal translation of 10.35 pixels, vertical translation of -20.78 pixels, rotation angle of 30.42 degrees and scale of 1.21. The transformation was estimated using the three algorithms under study. The results are shown in Figure 3 for both the T1 MRI image (left) and the Lena image (right). The results for Lena show that the correct translation can be found well under a standard deviation of 0.1, while the brain image can only achieve a correct transformation under a standard deviation of 0.07.

In another experiment, we tested the robustness of the method with respect to partial/missing data. For the first experiment, we used the Lena image, and replaced the pixel values within a circumference centered at the center of the transformed image with zeros, therefore reducing the amount of useful information. Figure 4(a) shows a plot of the log-TRME versus the percentage of deleted data (with respect to the total number of pixels) for four rigid transformations composed by $\phi = 30.42°$, $d_x = 10.35$, $d_y = -20.78$, and scaling factors of 0.8, 0.9, 1.0, and 1.1, respectively. We used different scales since a little variation in their values may affect significantly the amount of matchable pixel information. One can observe in this plot that in the case of scales less than 1.0, the TRME-values remain close to 0.01 even for images with 50% of missing data.
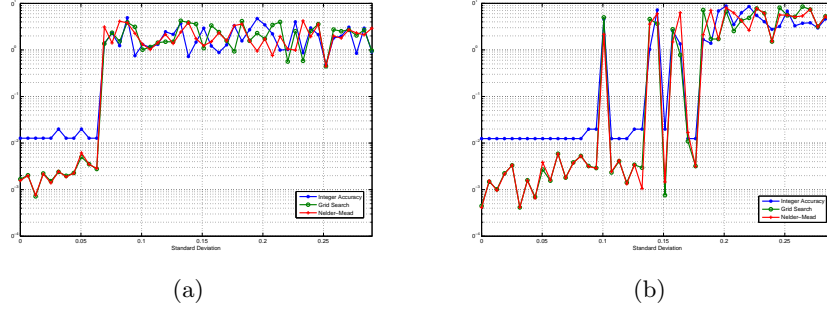
(a)   (b)

Fig. 3. Plots of the TRME with respect to the standard deviation of Gaussian noise added to the input images: (a) results with the T1 MRI image, (b) results with the Lena image.
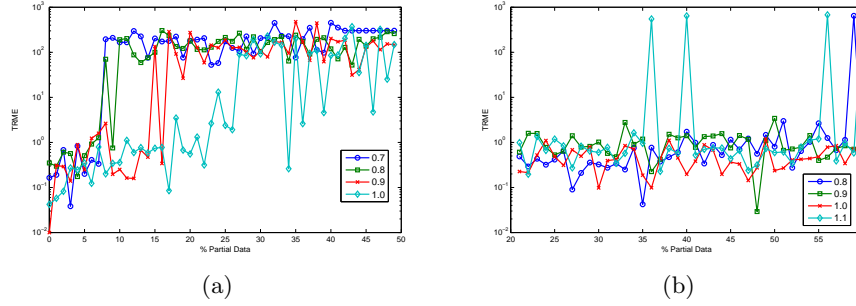

(a)   (b)

Fig. 4. Plots of the TRME with respect to the percentage of missing data. (a) results with the T1 MRI image, (b) results with the Lena image. Each trace corresponds to a different value of the scaling parameter (the rotation and translation parameters were fixed).

The experiment was repeated with the T1 MRI image shown in Fig. 1(a), and with scaling factors of 0.7, 0.8, 0.9, and 1.0. These results are shown in Figure 4(b). In this case, the matchable data does not cover the full image frame; therefore, the deletion of data from the center outwards has a bigger impact on the registration performance, especially when the scaling factor is small.

3.4   Results with real images

We also applied the proposed method to real image pairs where the true transformation is unknown. Figure 5 shows the result obtained from registering two 512×512 aerial images. Once the transformation was found, it was possible to build a larger map. Note that, in this case, the overlapping area between both images is relatively small (about one third of the image size), but the proposed method is still able to solve the problem accurately.
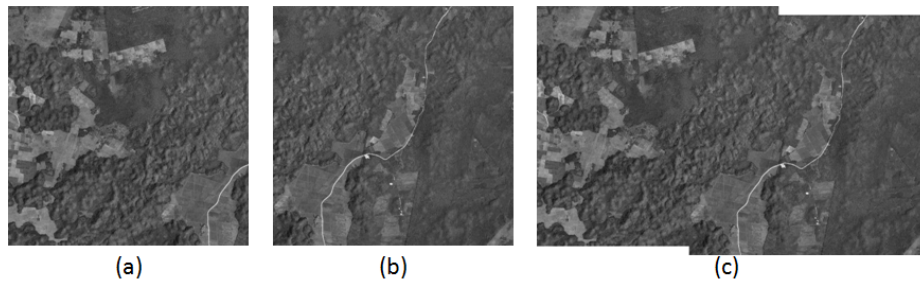
Fig. 5. Example of rigid registration of real images, where the true transformation is unknown. In this example, two aerial images are registered using the proposed method; once the transformation is found, the images can be stitched to form a larger map.

4 Conclusions

A novel approach to estimate the maxima of the phase-only correlation (POC) function was presented in this paper. This approach is based on minimizing the magnitude of the gradient of the POC, which can be done using heuristic techniques that rely only on the evaluation of the function to be minimized. The proposed method was applied to the rigid registration of two images, where it was evaluated in terms of precision and robustness to noise and missing data using synthetic examples. The results of these evaluations are favorable and demonstrate a significant improvement with respect to the classical phase correlation method where integer-valued translations are estimated. The registration algorithm was also applied to real image pairs where the true transformation is unknown, obtaining satisfactory results. A quantitative comparison between the proposed method and other state of the art methods for accurate estimation of the POC maxima is currently being performed. We are currently performing a comparative study between the proposed method and the most relevant techniques in the literature for the estimation of POC maxima with subpixel accuracy. Future work will focus on increasing the success rate of these methods for the rigid registration problem by analyzing multiple maxima of the phase correlation function.

References

1. Kuglin, C.D., Hines, D.C.: The Phase Correlation Image Alignment Method. Proc. of the IEEE Int. Conf. on Cybernetics and Society (1975) 163–165
2. De Castro, E., Morandi, C.: Registration of Translated and Rotated Images Using Finite Fourier Transforms. IEEE Transactions on Pattern Analysis and Machine Intelligence **9** (1987) 700–703
3. Reddy, B.S., Chatterji, B.N.: An FFT-Based Technique for Translation, Rotation, and Scale-Invariant Image Registration. IEEE Transactions on Image Processing **5** (1996) 1266–1271

4. Keller, Y., Averbuch, A., Moshe, I.: Pseudopolar-based estimation of large translations, rotations, and scalings in images. IEEE Transactions on Image Processing **14** (2005) 12–22
5. Keller, Y., Shkolnisky, Y., Averbuch, A.: The angular difference function and its application to image registration. IEEE Transactions on Pattern Analysis and Machine Intelligence **27** (2005) 969–976
6. Huang, J.Z., Tan, T.N., Ma, L., Wang, Y.H.: Phase correlation based iris image registration model. J. Comput. Sci. & Technol. **20** (2005) 419–425
7. Ito, K., Morita, A., Aoki, T., Higuchi, T., Nakajima, H., Kobayashi, K.: A fingerprint recognition algorithm using phase-based image matching for low-quality fingerprints. In: IEEE International Conference on Image Processing (ICIP 2005). (2005) (II) 33–36
8. Kolar, R., Sikula, V., Base, M.: Retinal image registration using phase correlation. In: Analysis of Biomedical Signals and Images (Proceedings of the 20-th International Eurasip Conference). (2010) 20: 244–252
9. Muquit, M.A., Shibahara, T., Aoki, T.: A High-Accuracy Passive 3D Measurement System Using Phase-Based Image Matching. IEICE Trans. Fundam. Electron. Commun. Comput. Sci. **E89-A** (2006) 686–697
10. Alba, A., Arce-Santana, E., Aguilar Ponce, R.M., Campos-Delgado, D.U.: Phase-correlation guided area matching for realtime vision and video encoding. Journal of Real-Time Image Processing **(in press)** (2012)
11. Takita, K., Muquit, M.A., Aoki, T., Higuchi, T.: A Sub-Pixel Correspondence Search Technique for Computer Vision Applications. IECIE Trans. Fundamentals **E87-A** (2004) 1913–1923
12. Chien, L.H., Aoki, T.: Robust Motion Estimation for Video Sequences Based on Phase-Only Correlation. 6th IASTED International Conference on Signal and Image Processing (2004) 441–446
13. Abdou, I.E.: Practical approach to the registration of multiple frames of video images. In: Proc. SPIE, Vol. 3653, Visual Communications and Image Processing '99. (1998) 371–382
14. Foroosh, H., Zerubia, J.B., Berthod, M.: Extension of phase correlation to subpixel registration. IEEE Transactions on Image Processing **11** (2002) 188–200
15. Takita, K., Aoki, T., Sasaki, Y., Higuchi, T., Kobayashi, K.: High-accuracy subpixel image registration based on phase-only correlation. IEICE Trans. Fundamentals **E86-A** (2003) 1925–1934
16. Nelder, J.A., Mead, R.: A simplex method for function minimization. Computer Journal **7** (1965) 308–313
17. Hoge, W.S.: A subspace identification extension to the phase correlation method. IEEE Transactions on Medical Imaging **22** (2003) 277–280
18. Arce-Santana, E., Alba, A.: Image registration using markov random coefficient fields. Lecture Notes in Computer Science **4958** (2008) 306–317